

# A Progressive Morphological Filter for Removing Nonground Measurements From Airborne LIDAR Data

Keqi Zhang, Shu-Ching Chen, *Member, IEEE*, Dean Whitman, Mei-Ling Shyu, *Member, IEEE*, Jianhua Yan, and Chengcui Zhang, *Student Member, IEEE*

**Abstract**—Recent advances in airborne light detection and ranging (LIDAR) technology allow rapid and inexpensive measurements of topography over large areas. This technology is becoming a primary method for generating high-resolution digital terrain models (DTMs) that are essential to numerous applications such as flood modeling and landslide prediction. Airborne LIDAR systems usually return a three-dimensional cloud of point measurements from reflective objects scanned by the laser beneath the flight path. In order to generate a DTM, measurements from nonground features such as buildings, vehicles, and vegetation have to be classified and removed. In this paper, a progressive morphological filter was developed to detect nonground LIDAR measurements. By gradually increasing the window size of the filter and using elevation difference thresholds, the measurements of vehicles, vegetation, and buildings are removed, while ground data are preserved. Datasets from mountainous and flat urbanized areas were selected to test the progressive morphological filter. The results show that the filter can remove most of the nonground points effectively.

**Index Terms**—Airborne laser altimetry, digital terrain model (DTM), light detection and ranging (LIDAR) data filtering.

## I. INTRODUCTION

HIGH-RESOLUTION digital terrain models (DTMs) are essential for many geographic information system (GIS)-related analysis and visualization. The airborne light detection and ranging (LIDAR) technology is revolutionizing our way to acquire a high-resolution DTM by allowing rapid and inexpensive measurements of topography over a large area. Airborne LIDAR systems usually obtain measurements for the horizontal coordinates ( $x, y$ ) and elevation ( $z$ ) of the reflective objects scanned by the laser beneath the flight path. These measurements generate a three-dimensional cloud of points with irregular spacing. The laser-scanned objects include buildings, vehicles, vegetation (canopy and understory), and “bare ground.” To generate a DTM, measurements from ground and nonground features have to be identified and classified.

Manuscript received July 28, 2002; revised October 29, 2002. This research was supported in part by Grant FEMA-DR-1249-FL from the Federal Emergency Management Agency.

K. Zhang and D. Whitman are with the International Hurricane Center, Florida International University, Miami, FL 33199 USA (e-mail: zhangk@fiu.edu; whitmand@fiu.edu).

S.-C. Chen, J. Yan, and C. Zhang are with the Distributed Multimedia Information System Laboratory, School of Computer Science, Florida International University, Miami, FL 33199 USA (e-mail: chens@cs.fiu.edu; jyan001@cs.fiu.edu; czhang02@cs.fiu.edu).

M.-L. Shyu is with the Department of Electrical and Computer Engineering, University of Miami, Coral Gables, FL 33124 USA (e-mail: shyu@miami.edu).

Digital Object Identifier 10.1109/TGRS.2003.810682

Removing nonground points from LIDAR datasets has proven to be a challenging task.

Kraus and Pfeifer [1], [2] utilized linear least squares interpolation iteratively to remove tree measurements and generate DTMs in forest areas. This method was extended later to filter buildings and trees in urban areas by Pfeifer *et al.* [3]. The iterative linear interpolation method removes a low-degree polynomial trend surface from the original elevation data to produce a set of reduced elevation values. This method requires that the reduced elevation follows a random process of ergodic property. However, this property is hard to satisfy in urban areas where significant anthropogenic modification of natural terrain occurs. Therefore, the iterative linear interpolation is not guaranteed to converge when being applied to LIDAR measurements for these areas.

Vosselman [4] proposed a slope-based filter that identifies ground data by comparing slopes between a LIDAR point and its neighbors. A point is classified as a ground measurement if the maximum value of slopes between this point and any other point within a given circle is less than a predefined threshold. The lower the threshold slope, the more objects will be removed. The threshold slope for a certain area is either constant or a function of distance. A reasonable threshold slope can be obtained by using prior knowledge about terrain in the study area.

There are two basic errors in classifying LIDAR measurements by virtually any filtering method. One is commission error that classifies nonground points as ground measurements [5]. The other is omission error that removes ground points mistakenly. The critical step in slope-based filtering is to determine an optimum threshold so that omission and commission errors can be minimized. Determining a slope threshold in terms of terrain information in the analyzed area is somewhat subjective. Vosselman [4] demonstrated that good results could be obtained by using threshold slopes from training datasets. However, the training datasets have to include all types of ground measurements in a study area to achieve good results, which is not always practical. Other attempts to improve the slope-based filter can be found in [6] and [7].

The implicit premise of applying the slope-based filter is that there is a distinct difference between the slope of terrain and that of nonground objects such as trees and buildings. Satisfactory results have been achieved in our experiments by applying the slope-based filter to flat urban areas such as Miami, FL. However, both omission and commission errors were large when this method was applied to vegetated mountain areas with a large slope variation.

Haugerud and Harding [8] developed an algorithm to filter tree points in forest areas by comparing local curvatures of point measurements. Ground measurements were selected by removing tree vertices iteratively from a triangulated irregular network (TIN) constructed from LIDAR measurements. Alternatively, ground points can be classified by iteratively selecting ground measurements from an original dataset. Axelsson [9] suggested adaptive TIN models to find ground points in urban areas. First, seed ground points within a user-defined grid of a size greater than the largest nonground features are selected to compose an initial ground dataset. Then, one point above each TIN facet is added to the ground dataset every iteration if its parameters are below threshold values. The iteration continues until no points can be added to the ground dataset. The problem with the adaptive TIN method is that different thresholds have to be given for various land cover types.

Another commonly used algorithm to remove nonground objects is a mathematical morphology filter which is applied to a grayscale image [4], [10], [11]. The elevation of trees, cars, and buildings is usually higher than those of surrounding ground points. If LIDAR points are converted into a regular, grayscale grid image in terms of elevation, then the shapes of buildings, cars, and trees can be identified by the change of gray tone. It is well known that compositions of algebraic set operations based on mathematical morphology can be used to identify objects in a grayscale image [12]. Therefore, mathematical morphology can be used to filter LIDAR data. The main objective of this paper is to develop a progressive morphology filter to enable automatic extraction of ground points from LIDAR measurements with minimal human interaction.

## II. MORPHOLOGICAL FILTERS

Mathematical morphology composes operations based on set theory to extract features from an image. Two fundamental operations, *dilation* and *erosion*, are commonly employed to enlarge (dilate) or reduce (erode) the size of features in binary images. Dilation and erosion operations may be combined to produce *opening* and *closing* operations. The concept of erosion and dilation has been extended to multilevel (grayscale) images and corresponds to finding the minimum or maximum of the combinations of pixel values and the kernel function, respectively, within a specified neighborhood of each raster [13].

These concepts can also be extended to the analysis of a continuous surface such as a digital surface model as measured by LIDAR data. For a LIDAR measurement  $p(x, y, z)$ , the dilation of elevation  $z$  at  $x$  and  $y$  is defined as

$$d_p = \max_{(x_p, y_p) \in w} (z_p) \quad (1)$$

where points  $(x_p, y_p, z_p)$  represent  $p$ 's neighbors (coordinates) within a window,  $w$ . The window can be a one-dimensional (1-D) line or two-dimensional (2-D) rectangle or other shapes. The dilation output is the maximum elevation value in the neighborhood of  $p$ . Erosion is a counterpart of dilation and is defined as

$$e_p = \min_{(x_p, y_p) \in w} (z_p). \quad (2)$$

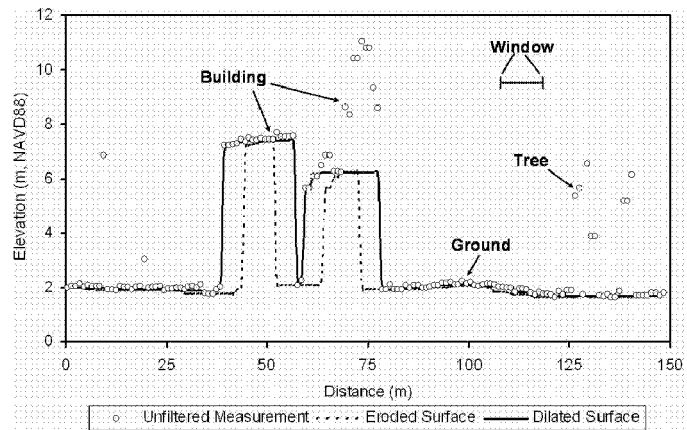


Fig. 1. Unfiltered and filtered LIDAR measurements along a profile at the Florida International University campus. The unfiltered points are sampled every  $1 \times 1 \text{ m}^2$  cell along the profile. If more than one measurement falls within a cell, the point with the minimum elevation is selected. If there is no measurement for a cell, nearest neighborhood interpolation is used to derive an elevation. The filtered data are obtained by applying an opening operation with a window size of 11 m. The profile location is shown in Fig. 5. Note tree objects less than the window size are removed by erosion, while the large building objects are restored by the dilation.

The combination of erosion and dilation generates opening and closing operations that are employed to filter LIDAR data. The opening operation is achieved by performing an erosion of the dataset followed by a dilation, while the closing operation is accomplished by carrying out a dilation first and then an erosion. Fig. 1 shows the result of performing an opening operation using a line window. As the result demonstrates, an erosion operation removed tree objects of sizes smaller than the window size, while the dilation restored the shapes of large building objects. The ability of an opening operation to preserve features larger than the window size is very useful in some applications. For example, the measurements of cliff edges can be preserved if the morphological filters are applied to the LIDAR measurements for rocky coasts.

Kilian *et al.* [10] proposed a method to remove nonground points using a morphological filter. In their method, a point with the lowest elevation within a given window size is first detected after an opening operation is performed on the dataset. Then the points in this window that fall within a band above the lowest elevation are selected as ground points. The range of the band is determined by the accuracy of the LIDAR survey, which is normally 20–30 cm. All ground points are identified by moving the filtering window over the entire dataset.

The selection of a filtering window size and the distribution of the buildings and trees in a specific area are critical for the success of this method. If a small window size is used in Kilian's method, most of the ground points will be preserved. However, only small nonground objects such as cars and trees will be effectively removed. The points corresponding to the tops of large-sized building complexes that often exist in urban areas cannot be removed. The risk of making commission errors is high. On the other hand, the filter tends to over-remove the ground points with a large window size. For example, road surface points next to drainage canals will be removed completely if the window size is larger than the width of a road. In addition, the tops of local mounds and sand dunes in flat coastal areas

are often “chopped off” by using a large size window. Ideally, the window size of the morphological operation should be small enough to preserve all ground details and large enough to remove buildings, cars, and trees. Unfortunately, an ideal window size does not exist in the real world.

To avoid this conflict, Kilian *et al.* [10] proposed to apply the operations with different window sizes to the dataset several times starting from the smallest size. Each point is assigned a weight related to the window size provided it is classified as a ground point. The larger the window size of an operation, the higher the weight of a point. Finally, the terrain surface is estimated by using all the survey points with assigned weights. Although a better terrain surface could be derived using the weighted points from different sizes of morphological operations, this method does not make the improvement in separating ground and nonground LIDAR measurements at the point level. Classifying ground and nonground measurements at the point level is useful for some applications.

Lohmann *et al.* [11] used a dual-rank morphological filter proposed by Eckstein and Munkelt [14] to classify LIDAR point data. The dual-rank filter initially sorts the neighborhood of a point  $p$  in terms of elevation, and then selects an elevation with a given rank value  $i$  to perform a rank operation  $R(p, i)$ , where  $i$  ranges from 1 to  $n_p$ , and  $n_p$  is the total number of points of  $p$ 's neighbors (including  $p$ ). The neighbors of a point are delineated by a window that is usually a circle and can be any shape. The dual-rank filter is then defined as

$$DR(p, i) = R(p, i) \circ R(p, n_p - i + 1). \quad (3)$$

The symbol “ $\circ$ ” indicates the successive operations: the points are processed by the first rank operation, and then the second rank operation is performed on the results from the first operation. The dual-rank filter becomes an opening operation when the rank value is one (i.e.,  $i = 1$ ) and closing operation when the rank value is  $n_p$  ( $i = n_p$ ). Promising results have been achieved by applying a dual-rank filter to a test dataset [11]. However, an optimum filtering window is hard to derive because a single fixed-size window of the dual-rank filter cannot fit all nonground objects.

The above morphological filters need to be improved because they suffer from various problems such as the requirement of a predefined filtering window size. In addition, a highly automatic filtering tool that identifies ground measurements is desired due to the large volume of LIDAR data involved. Furthermore, separating ground and nonground measurements at the point level is preferred so that users can generate a DTM using the interpolation method that fits their applications best. The focus of this study is to develop a morphological filter can remove nonground measurements from LIDAR dataset at the point level.

### III. PROGRESSIVE MORPHOLOGICAL FILTER

It has been shown that morphological filters can remove measurements for buildings and trees from LIDAR data [10], but it is difficult to detect all nonground objects of various sizes using a fixed filtering window size. This problem can be solved by increasing window sizes of morphological filters gradually.

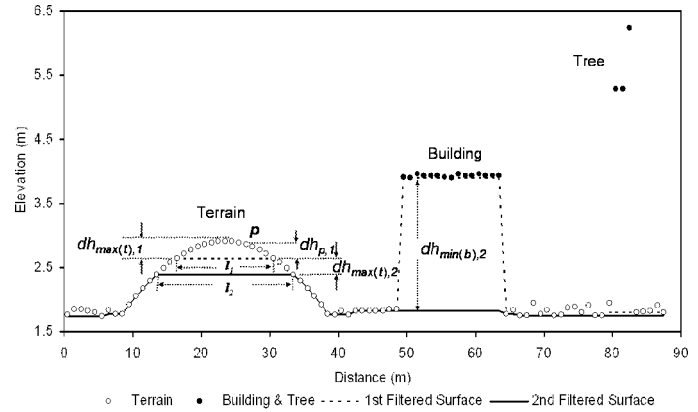


Fig. 2. Process of the progressive morphological filter to identify terrain and building measurements. The dots represent synthetic points based on LIDAR surveys. The first filtered elevation surface (dashed line) is obtained by applying an opening operation with a window size of 15 m ( $l_1$ ) to the raw point data. The second filtered elevation surface (solid line) is derived by applying an opening operation with a window size of 21 m ( $l_2$ ) to the first filtered surface.

Fig. 2 illustrates the process of a progressive morphological filter. An initial filtered surface is derived by applying an opening operation with a window of length  $l_1$  to the raw data. The large nonground features such as buildings are preserved because their sizes are larger than  $l_1$ , while individual trees of size smaller than  $l_1$  are removed. For the terrain, features smaller than  $l_1$  are cut off and replaced by the minimum elevation within  $l_1$ .

In the next iteration, the window size is increased to  $l_2$ , and another opening operation is applied to the filtered surface, resulting in a further smoothed surface. The building measurements are removed and replaced by the minimum elevation of previous filtered surface within  $l_2$ , since the size of the building is smaller than the current window size.

By performing an opening operation to laser-scanned data with a line window that increases in size gradually, the progressive morphological filter can remove buildings and trees at various sizes from a LIDAR dataset. However, the filtering process tends to produce a surface that lies below the terrain measurements, leading to incorrect removal of the measurements at the top of high-relief terrain (points above  $l_2$  in Fig. 2). Even in the flat ground areas, the filtered surface is usually lower than the original measurements. Therefore, most point measurements for terrain are removed, and only a filtered surface is available if the opening operation is performed to the LIDAR data directly. This problem can be overcome by introducing an elevation difference threshold based on elevation variations of the terrain, buildings, and trees.

Each building has a certain size and height. There is an abrupt change in elevation between the roof and base of a building, while the elevation changes of terrain are gradual (Fig. 2). The difference in the elevation variations of buildings and terrain can help the filter to separate the building and ground measurements. Suppose that  $dh_{p,1}$  represents the height difference between an original LIDAR measurement and the filtered surface in the initial iteration at any given point  $p$  (Fig. 2), and  $dh_{T,1}$  represents the elevation difference threshold. Point  $p$  is classified as a ground measurement if  $dh_{p,1} \leq dh_{T,1}$  and as a nonground measurement if  $dh_{p,1} > dh_{T,1}$ . Let  $dh_{\max(t),1}$  stand for the

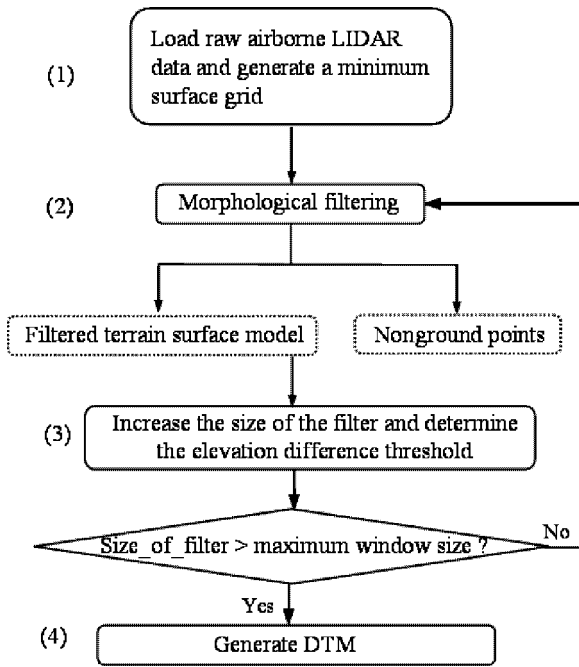


Fig. 3. Framework of the progressive morphological filter.

maximum height difference between the original terrain measurements and the filtered surface (Fig. 2). If a  $dh_{T,1}$  is selected such that the  $dh_{\max(t),1}$  is less than  $dh_{T,1}$ , then the LIDAR measurements for terrain will be preserved. In general,  $dh_{T,1}$  will be a function of window size. How to derive this threshold value will be discussed later.

In the second iteration, suppose that the maximum height difference between the previous and this filtered terrain surface is  $dh_{\max(t),2}$ . The ground measurements within  $dh_{\max(t),2}$  will be preserved as long as  $dh_{\max(t),2}$  is smaller than the elevation difference threshold  $dh_{T,2}$  for the current operation. Suppose that the minimum elevation difference for the building between the previous and current filtering operation is represented by  $dh_{\min(b),2}$ , which is approximately the height of the building. The building measurements will be removed on condition that  $dh_{\min(b),2}$  is larger than  $dh_{T,2}$ .

Generally, the elevation difference threshold  $dh_{T,k}$  is set to be the minimum height value of the building objects in an analyzed area at iteration  $k$ . Taking  $dh_{T,k}$  as the threshold, for any given point  $p$  at  $k$ th opening operation, we mark  $p$  as a ground measurement if  $dh_{p,k} \leq dh_{T,k}$ , and as a nonground measurement otherwise. In this way, the measurements for buildings with various sizes can be identified by gradually increasing the window sizes and applying an opening operation repeatedly until a window size is greater than the size of the largest building. Since there is also an abrupt elevation change from trees to adjacent ground, the above building filtering procedure can be applied to the removal of tree measurements as well. Note that the filtered surfaces from the opening operation are not utilized to generate the DTM, but used to help classify point measurements together with elevation difference thresholds.

The detailed steps to use the progressive morphological filter to construct the DTMs are shown in Fig. 3 and given as follows.

Step 1: The irregularly spaced  $(x, y, z)$  LIDAR measurements are loaded. A regularly spaced minimum surface grid is constructed by selecting the minimum elevation in each grid cell. Point coordinates  $(x, y, z)$  are stored in each grid cell. If a cell contains no measurements, it is assigned the value of nearest point measurement.

Step 2: The progressive morphological filter whose major component is an opening operation is applied to the grid surface. At the first iteration, the minimum elevation surface together with an initial filtering window size provide the inputs for the filter. In the following iterations, the filtered surface obtained from the previous iteration and an increased window size from Step 3 are used as input for the filter. The output of this step include a) the further smoothed surface from the morphological filter and b) the detected nonground points based on the elevation difference threshold.

Step 3: The size of the filter window is increased and the elevation difference threshold is calculated. Steps 2 to 3 are repeated until the size of the filter window is greater than a predefined maximum value. This value is usually set to be slightly larger than the maximum building size.

Step 4: The last step is to generate the DTMs based on the dataset after nonground measurements have been removed.

Note that each cell of the minimum surface grid generated in Step 1 contains an original or interpolated LIDAR point with elevation representing the cell value. Any filtering operation performed to the grid is actually applied to points in cells. Therefore, the progressive morphological filter classifies the LIDAR measurements at the point level.

#### IV. PARAMETERS FOR PROGRESSIVE MORPHOLOGICAL FILTER

The selection of the window size and elevation difference threshold is critical to achieve good results when applying the morphological filter. For window size selection, one straightforward choice is to increase the window size linearly by the following formula:

$$w_k = 2kb + 1 \quad (4)$$

where  $k = 1, 2, \dots, M$ , and  $b$  is the initial window. The maximum window size (number of cells) is equal to  $2Mb + 1$ . Taking  $2kb + 1$  as the window size guarantees that the filter window is symmetric around the central point so that the programming of the opening operation is simplified. The advantage of increasing the window size linearly is that gradually changing topographic features are well preserved. However, considerable computing time is needed for an area with large nonground objects.

Alternatively, the window size can be increased exponentially to reduce the number of iterations used in the filter.

$$w_k = 2b^k + 1 \quad (5)$$

where  $b$  is the base of an exponential function;  $k = 0, 1, 2, \dots, M$ ; and again  $2b^M + 1$  is equal to the maximum window size.

The elevation difference threshold can be determined based on the slope of topography in the study area. There is a relationship between the maximum elevation difference  $dh_{\max(t),k}$  for the terrain, window size  $w_k$ , and the terrain slope  $s$  (Fig. 2) assuming that the slope is constant.

$$s = \frac{dh_{\max(t),k}}{\frac{(w_k - w_{k-1})}{2}}. \quad (6)$$

Therefore, the elevation threshold  $dh_{T,k}$  is given by

$$dh_{T,k} = \begin{cases} dh_0, & \text{if } w_k \leq 3 \\ s(w_k - w_{k-1})c + dh_0, & \text{if } w_k > 3 \\ dh_{\max}, & \text{if } dh_{T,k} > dh_{\max} \end{cases} \quad (7)$$

where  $dh_0$  is the initial elevation difference threshold;  $s$  is the slope;  $c$  is the cell size; and  $dh_{\max}$  is the maximum elevation difference threshold.

In urban areas, primary nonground objects include cars, trees, and buildings. The sizes of individual cars and trees are much less than that of the buildings, so most of them are often removed in the first several iterations, while the large buildings will be removed last. The maximum elevation difference threshold  $dh_{\max}$  can be set to a fixed height (e.g., the lowest building height) to ensure that building complexes are identified. The optimum  $s$  is usually achieved by iteratively comparing the filtered and unfiltered data. On the other hand, the nonground objects in the mountainous areas are primarily vegetation (trees). There is no need to set up a fixed maximum elevation difference threshold to remove trees, and  $dh_{\max}$  is usually set up as the largest elevation difference in the study area.

## V. ALGORITHM AND IMPLEMENTATION

The progressive morphological filter can be either 1- or 2-D depending on its window shape. The filter is 2-D if its window is a 2-D shape such as rectangle or circle, while the filter is 1-D if its window is defined by a segment of a line. The algorithms for 1- and 2-D filters are similar. For simplicity, yet not losing generality, only the input, output and algorithm for the 1-D progressive morphological filter are presented as follows.

### Algorithm 1: The progressive morphological filtering algorithm

#### Input:

- o A set of points representing LIDAR measurements. Each point has three components ( $x$ ,  $y$ , and  $z$ ) to represent horizontal coordinates and elevation of a LIDAR measurement.
- o Cell size  $c$ .
- o Parameter  $b$  in (4) or (5).
- o Maximum window size.
- o Terrain slope  $s$ .
- o Initial elevation difference threshold  $dh_0$ .
- o Maximum elevation difference  $dh_{\max}$ .

#### Output:

- o Two sets of the classified points representing ground and nonground measurements.
1. Determine the minimum and maximum  $x$  and  $y$  values.

2. Determine the numbers of rows ( $m$ ) and columns ( $n$ ) using  $m = \text{floor}[(\max(y) - \min(y))/c] + 1$  and  $n = \text{floor}[(\max(x) - \min(x))/c] + 1$ .
3. Create a 2-D array  $A[m, n]$  for LIDAR points,  $p(x, y, z)$ . Traverse every point to determine the cell in which the point will fall according to its  $x$  and  $y$  coordinates. If more than one point falls in the same cell, select the one with minimum elevation.
4. Interpolate elevation of cells in  $A$  which do not contain any points using the nearest neighbor method. Set the  $x$  and  $y$  coordinates of those interpolated cells as zero to distinguish them from those cells that contain LIDAR points. Copy  $A$  to  $B$ . Initialize elements of a 2-D integer array  $\text{flag}[m, n]$  with 0.
5. Determine series of  $w_k$  using (4) or (5), where  $w_k \leq$  maximum window size.
6.  $dh_T = dh_0$
7. for each window size  $w_k$
8. for  $i = 1$  to  $m$
9.  $P_i = A[i;]$  ( $A[i;]$  represents a row of points at row  $i$  in  $A$  and  $P_i$  is a 1-D array)
10.  $Z \leftarrow P_i$  (Assign elevation values from  $P_i$  to a 1-D elevation array  $Z$ )
11.  $Z_f = \text{erosion}(Z, w_k)$
12.  $Z_f = \text{dilation}(Z_f, w_k)$
13.  $P_i \leftarrow Z_f$  (Replace  $z$  values of  $P_i$  with the values from  $Z_f$ )
14.  $A[i;] = P_i$  (Put the filtered row of points  $P_i$  back to row  $i$  of array  $A$ )
15. for  $j = 1$  to  $n$
16. if  $Z[j] - Z_f[j] > dh_T$  then  $\text{flag}[i, j] = w_k$
17. end for  $j$  loop
18. end for  $i$  loop
19. if  $(dh_T > dh_{\max})$
20.  $dh_T = dh_{\max}$
21. else
22.  $dh_T = s(w_k - w_{k-1})c + dh_0$
23. end for window size loop
24. for  $i = 1$  to  $m$
25. for  $j = 1$  to  $n$
26. if  $(B[i, j](x) > 0$  and  $B[i, j](y) > 0)$
27. if  $(\text{flag}[i, j] = 0)$
28.  $B[i, j]$  is a ground point
29. else
30.  $B[i, j]$  is a nonground point
31. end for  $j$  loop
32. end for  $i$  loop

#### Erosion( $Z, w_k$ ):

1. for  $j = 1$  to  $n$
2.  $Z_f[j] = \min_{j-[w_k/2] < i < j + [w_k/2]} (Z[i])$
3. return  $Z_f$

#### Dilation( $Z, w_k$ ):

1. for  $j = 1$  to  $n$
2.  $Z_f[j] = \max_{j-[w_k/2] < i < j + [w_k/2]} (Z[i])$
3. return  $Z_f$



Fig. 4. Aerial photograph for the University Park campus of FIU. Six hundred forty-eight random sample points are also overlain over the photograph. The ground and nonground measurements identified from these samples by the progressive morphological filter are represented by white and black dots, respectively. The white rectangles represent the range of Figs. 5 and 6.

The above 1-D erosion algorithm can be easily extended to a 2-D one with a square window by performing erosion in the  $x$  direction first and then in the  $y$  direction. The same rule can be applied to dilation as well.

The major computation time needed by the progressive morphology filter is the erosion and dilation in addition to the interpolation. It is easy to see that the opening algorithm requires  $O(wN)$  time to perform an erosion and dilation, where  $w$  is the window size of the morphological filter and  $N$  is the product of the number of rows and columns for an array ( $A$ ) holding LIDAR data. For  $M$  windows, the time complexity is equal to

$$O\left(\sum_{k=1}^M w_k N\right). \quad (8)$$

## VI. TEST DATASETS

The morphological filter was tested on two LIDAR datasets: an urban setting with low-relief topography and a forested section with high-relief topography. The urban test site is located at the Florida International University (FIU) campus in Miami, FL and covers about  $1.8 \text{ km}^2$ . There are residential houses, large buildings, single trees, forests, parking lots, open ground, ponds, roads, a major highway, and a canal in this area (Fig. 4). The overall slope of the terrain is gentle except for several small mound areas. The dataset was collected by an Optech ALTM 1210 LIDAR mapping system mounted to a Cessna 337 aircraft in April 2000. By flying at a speed of 200 km/h, altitude of 600 m, off-nadir scan angle of  $18^\circ$ , and laser repetition rate of 10 000 pulses per second, we collected a 400-m-wide swath of laser range data. The objects were measured by a 15-cm footprint spaced approximately 2 m apart. Flight lines were spaced 300 m apart to avoid possible data gaps.

The test dataset for the high-relief area came from the Puget Sound LIDAR Consortium (<http://www.pugetsoundlidar.org>).

TABLE I  
PARAMETERS FOR THE PROGRESSIVE MORPHOLOGICAL FILTER. BOTH FIU CAMPUS AND PUGET SOUND ARE IN METERS

Location	FIU Campus	Puget Sound
Cell size ( $c$ in Equation (7))	1	1
Base of the exponential window ( $b$ in Equation (5))	2	2
Increment step for windows ( $k$ in Equation (5))	0, 1, 2, ..., 8	0, 1, 2, ..., 5
Slope ( $s$ in Equation (7))	0.08	1.2
Initial threshold ( $dh_0$ in Equation (7))	0.25	0.2
Maximum threshold ( $dh_{\max}$ in Equation (7))	2.5	210

The site consists of  $1.3 \text{ km}^2$  of tree-covered mountain land. The distribution of trees varies with topography, and usually is dense in the valleys and sparse on the ridges. The terrain varies considerably with slopes ranging from 0.1 to 1.5. The LIDAR data were derived using TerraPoint LLC's laser altimeter, and the dataset includes up to four returns for each laser pulse. Each flight surveyed a 600-m-wide swath with a 0.9 m-diameter laser footprint spaced approximately every 1.5 m. An average point density of one point per square meter was derived by measuring the area with a 50% side-lap between swaths.

## VII. RESULTS

A progressive morphological filter was applied to two test LIDAR datasets to examine its filtering effect. The opening operation was applied to both  $x$  and  $y$  directions at every step to ensure that the nonground objects were removed. The filtering parameters used in our experiments are listed in Table I. The



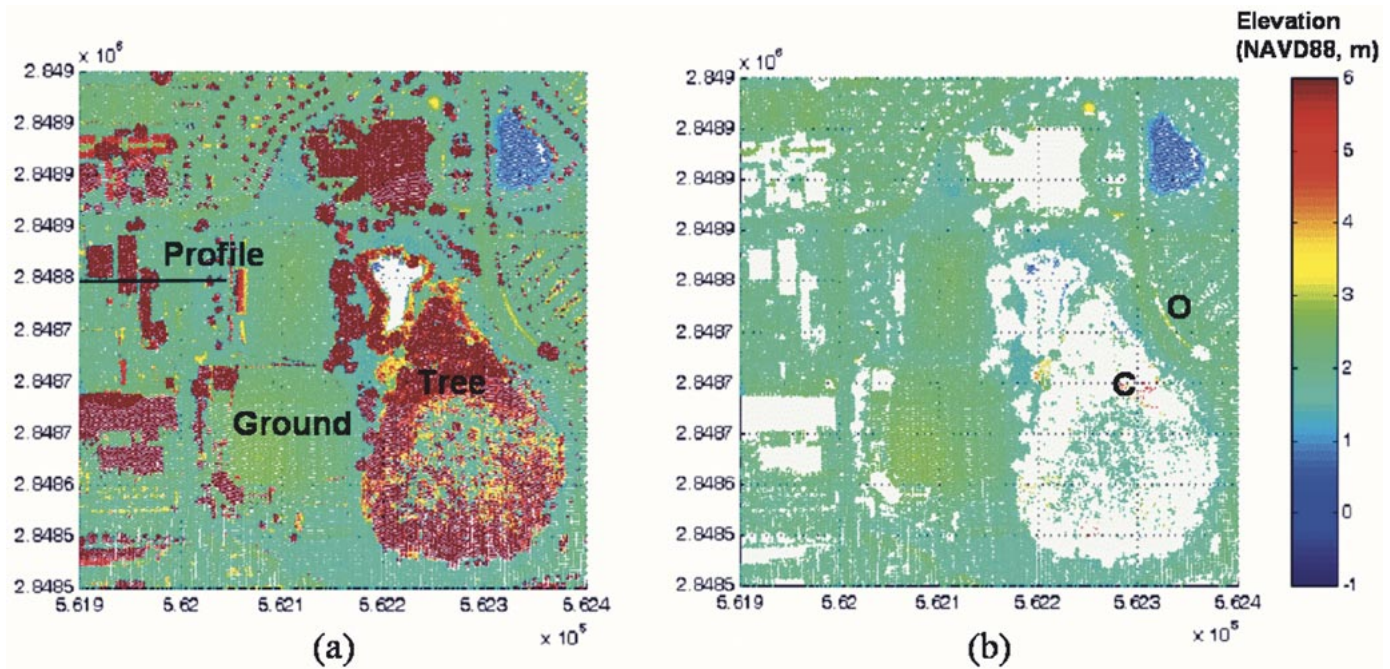


Fig. 5. (a) Unfiltered and (b) filtered LIDAR point measurements for an area at the FIU campus with cars, single trees, buildings, and a small forest. The elevation values higher than 6 m were assigned the same color (red) for display purposes. The horizontal coordinates ( $x$  and  $y$ ) are in UTM zone 17 referenced to NAD83. Elevation ( $z$ ) coordinates are referenced to NAVD88. The map units are in meters. Note that the filter removed most of the nonground objects successfully, but some tree measurements (C) were not removed completely, and some ground points were filtered out mistakenly (O).

window size was incremented using the exponential function [as defined in (5)].

For the FIU campus dataset, the initial  $dh_0$  was set up as 0.25 m, which is approximately equal to the LIDAR measurement error (0.2–0.3 m). The cell size  $c$  was set to 1 m, which is about two times less than the average spacing between LIDAR measurements, and therefore most of the LIDAR points were preserved when a grid was generated for the filter. A small slope factor (0.08) was selected to filter this urban dataset with nearly flat terrain. A 2.5-m maximum elevation difference threshold was used to ensure the removal of the buildings.

There are about 1.03 million LIDAR measurements for this area and the number of grid cells to hold the data is 2.02 million. Among them, 0.71 million cells have data, and about 30% of the points were removed as repeated measurements for each cell. About 74% of the points in cells having data were classified as ground measurements by the progressive morphological filter.

For the high-relief test area, the initial  $dh_0$  was selected to be 0.2 m, and maximum elevation difference threshold was set to be the largest elevation difference value in the analyzed area. The terrain slopes of the Puget Sound area in Washington State are relatively steep, ranging from 0.1 to 1.5, and therefore, the  $s$  in (7) was set to 1.2, which is close to the maximum slope.

There are about 2.68 million LIDAR measurements for the mountain area, and the number of grid cells to hold the data is 1.4 million. Among them, only 0.91 million cells have data, and about 76% of the points were removed as repeated measurements for each cell because this dataset includes multireturns of the same laser pulse. Fifty-eight percent of the points in cells having data were classified as ground measurements by the filter.

### VIII. ACCURACY ANALYSIS

Like other filtering methods, the progressive morphological filter is subject to omission and commission errors. In order to measure the effectiveness of the filter, these two errors have to be examined. Both qualitative and quantitative methods were employed in this study. A qualitative method checks whether nonground features such as buildings are excluded entirely and whether ground features like small mounds are included completely by visually comparing the unfiltered and filtered data. The quantitative method examines the correctness of the filtered measurements at the point level from a random sample.

The raw LIDAR data, filtered measurements, black-and-white aerial orthophotographs, and field investigation were used to quantitatively examine the filtering errors for the FIU campus dataset. The aerial photographs were collected in 1999 at a resolution of 0.3 m. The evergreen vegetation at the FIU campus changes little through time. Therefore, vegetation and building information from aerial photographs can be used to help identify filtering errors, although the aerial photographs were taken at the time different from the LIDAR surveying. Quantitative analysis of filtering accuracy for the mountain dataset was not performed because the aerial photographs for the study area are not available, and it is too expensive to do a field examination.

Fig. 5(a) and (b) shows the unfiltered and filtered LIDAR measurements for an area occupied with cars, single trees, buildings, a small forest, and ground. As can be seen from Fig. 5, most of the cars, trees, and buildings were removed successfully by the filter. However, some commission and omission errors did occur. A few measurements for trees remained [C in



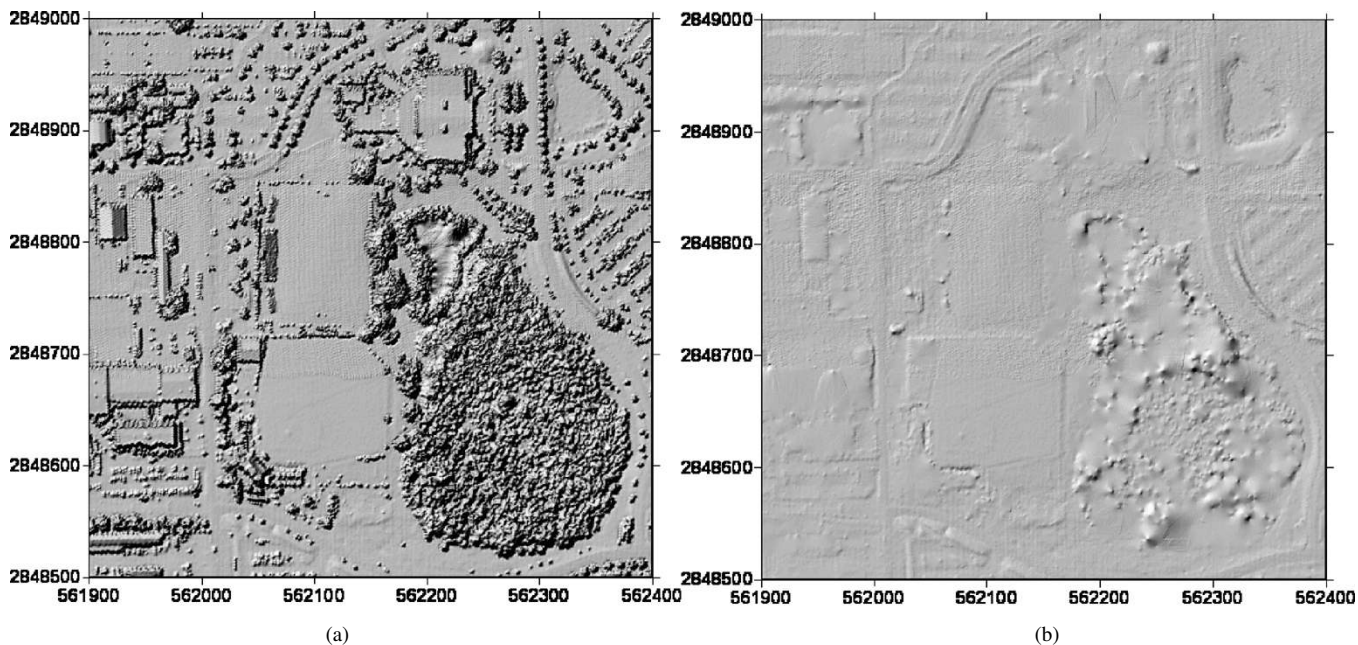


Fig. 6. Shaded relief maps for the grids generated from (a) unfiltered and (b) filtered LIDAR data from the FIU campus. The grids of cell size 0.5 m were generated by applying Kriging interpolation to LIDAR data with a search radius of 100 m in the Surfer software program. Note the effect of the remaining tree points in the filtered data on the DTM (b).

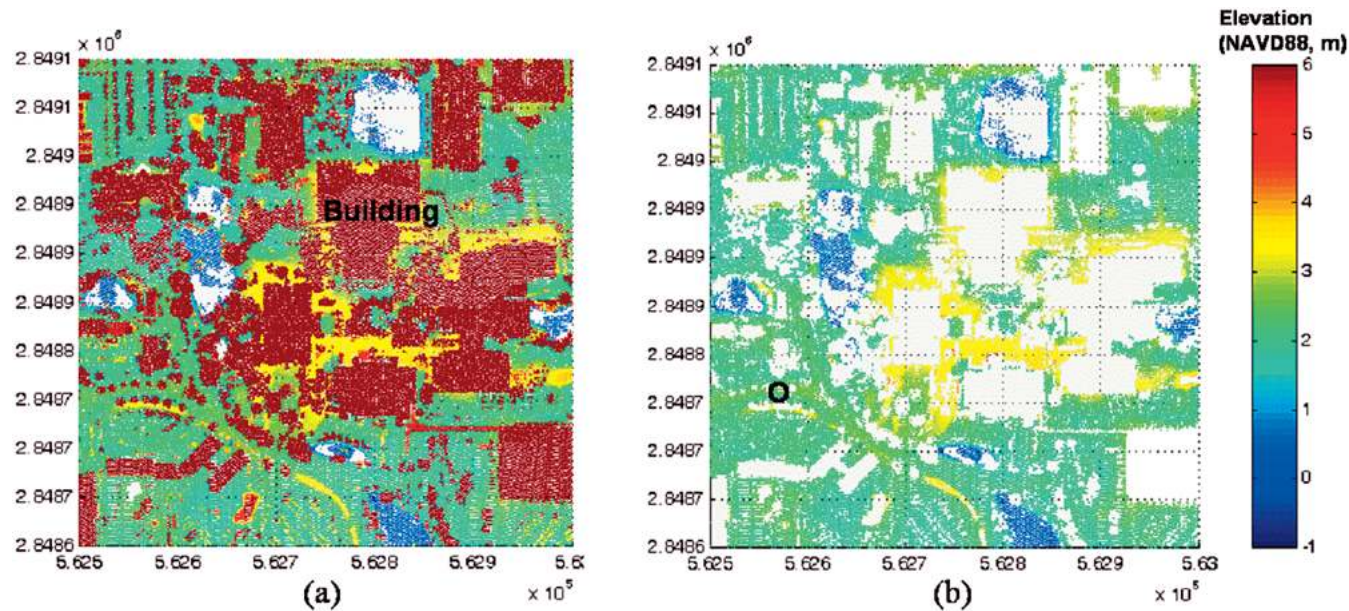


Fig. 7. (a) Unfiltered and (b) filtered LIDAR point measurements for an area at the FIU campus with many buildings. The buildings were removed by the filter completely, but some omission errors occurred (O).

Fig. 5(b)], and a small mound was mistakenly removed [O in Fig. 5(b)]. The first error occurs because of the high tree density surrounding C [Fig. 5(a)]. Few true ground LIDAR measurements were derived because most laser pulses were reflected by the canopy and did not reach the ground. The elevation changes of some tree tops are similar to those of low topographic relief. Fig. 6 shows the shaded relief maps for the grids generated from unfiltered and filtered LIDAR data using Kriging interpolation [15]. The effect of commission errors on the DTM in the forest area is obvious [Fig. 6(b)]. The reason for the omission of the small mounds is that the slopes of these mounds are relatively steep, which is larger than  $s$  in (7).

Figs. 7 and 8 show the unfiltered and filtered LIDAR point measurements and shaded relief grid maps for a dense building area at the FIU campus. In general, the progressive morphological filter performed well in this area. Omission errors occurred in a few spots because of the complicated composition of buildings and ground objects [O in Fig. 7(b)].

A simple random sampling scheme [16] was employed to select the points to quantitatively examine omission and commission errors of the filtering results for the FIU campus dataset. First, 1600 random points were generated within a rectangle of 2000 m long ( $x$  or east–west direction) and 800 m wide ( $y$  or north–south direction), which is the extent of the LIDAR dataset.



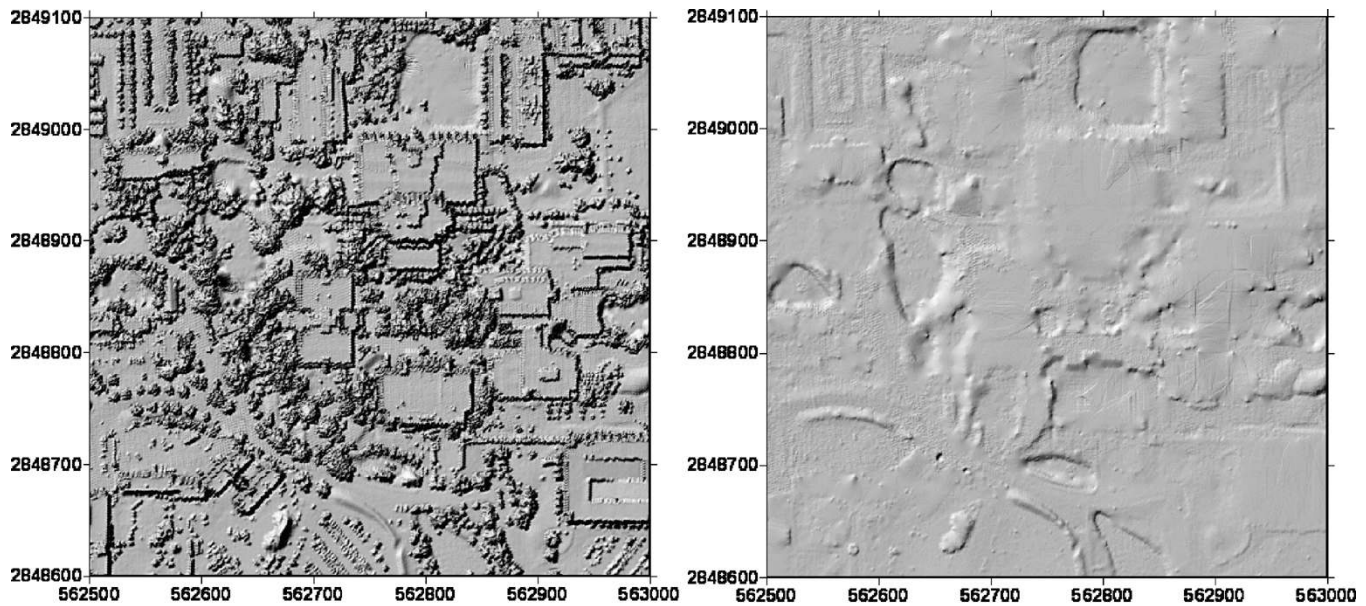


Fig. 8. Shaded relief maps of two grids from unfiltered and filtered LIDAR data with many buildings at FIU campus. Grids of 0.5-m cell size were generated using Kriging interpolation with a search radius of 100 m.

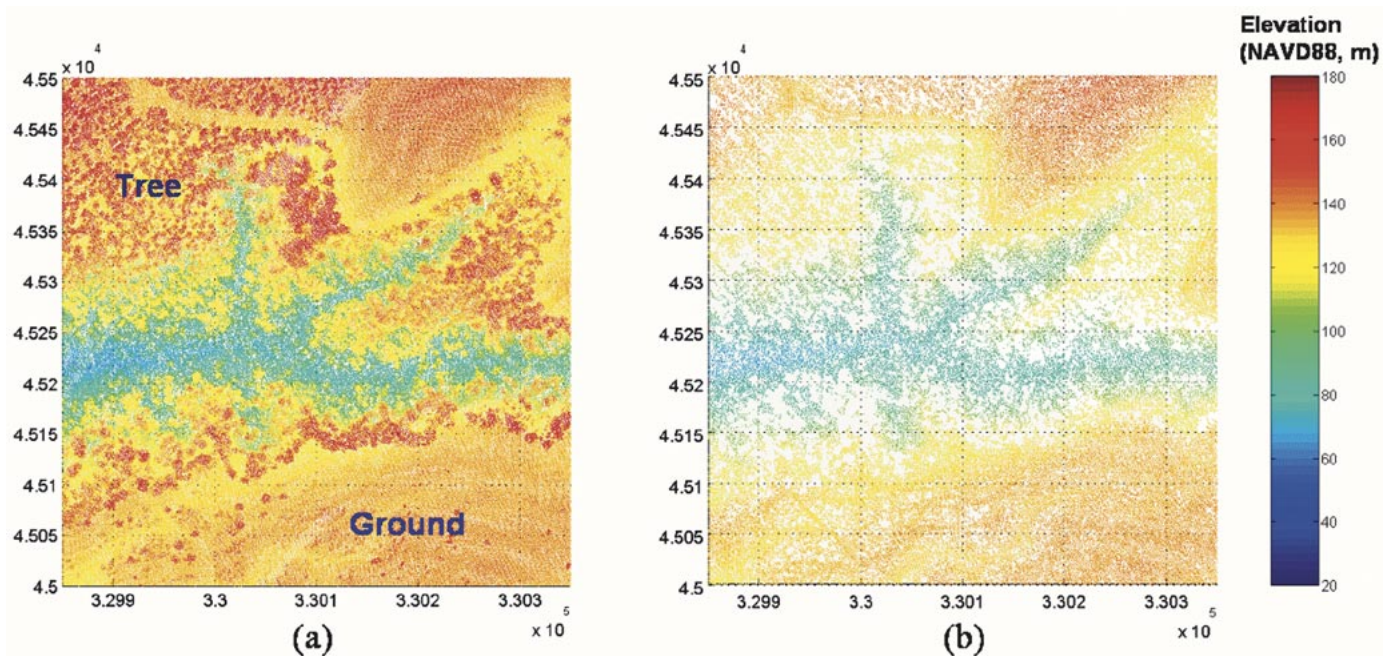


Fig. 9. (a) Unfiltered and (b) filtered LIDAR measurements for mountains at Puget Sound, Washington State. The unfiltered data include all-return LIDAR measurements. The horizontal coordinates are in Washington State plane north coordinate system and refer to datum NAD83. Elevations refer to NAVD88. All coordinate units are meters. The trees were removed from the LIDAR dataset, while the ground measurements were well preserved.

Second, the row and column locations of those 1600 samples in array  $B$ , which holds a minimum elevation grid of 1 m cell size interpolated from the unfiltered LIDAR dataset (Step 4 in Algorithm 1), were determined based on their  $x$  and  $y$  coordinates. Third, 648 cells of the grid were derived by removing those sample cells which do not have LIDAR measurements. Fourth, the ground measurements in the 648 cells were marked as 1, and the nonground points were marked as 0 in terms of filtering results. Finally, the 648 measurements were manually examined point by point to find the filtering errors by overlaying them into the aerial photographs (Fig. 4) and a digital surface model in Ar-

cGIS. The digital surface model with cell size of 0.5 m was generated by applying Kriging interpolation to the raw LIDAR measurements. All errors detected from overlay analysis were further examined in the field to avoid possible misinterpretation.

Quantitative error analysis shows that there were 17 omission and two commission errors in 648 samples, about 3% of the total, indicating that the progressive morphological filter works well. One reason for having more omission errors than commission errors is that the parameters were set up in such a way that the filter can remove most of the nonground measurements. The other reason is that the samples are not dense enough to pick up

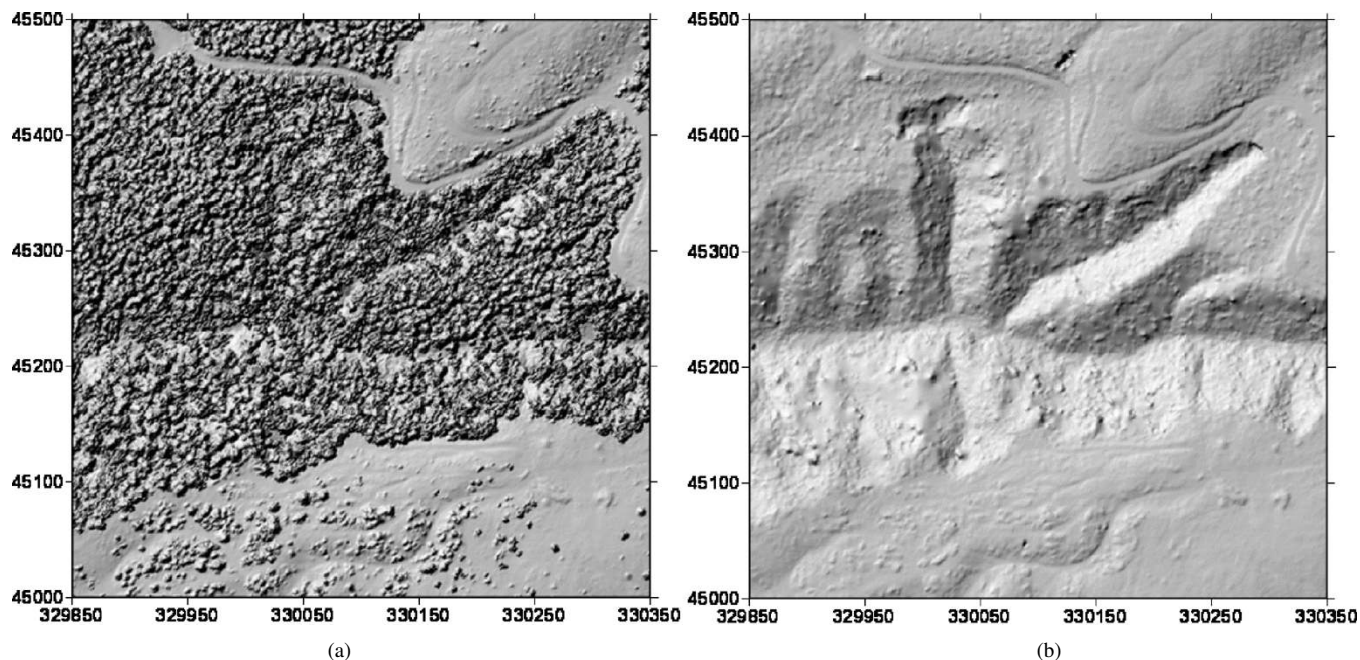


Fig. 10. Shaded relief maps for two grids generated from (a) unfiltered and (b) filtered data at the Puget Sound area, Washington State. The topography of valleys is clear, and linear features such as roads are well preserved in the filtered image.

the scattered commission errors in small areas [C in Fig. 5(b)]. Sample size and sampling scheme can affect the error analysis considerably [5]. The effect of various sample sizes and sampling schemes such as stratified random sampling on accuracy analysis of the filtering results needs to be studied further in the future.

Comparison of Fig. 9(a) and (b) shows that tree measurements were well removed, while ground points were preserved in the high-relief test area. The shaded relief maps [Fig. 10(a) and (b)] for the two grids generated from unfiltered and filtered data illustrate that the topography of valleys is much clear in the filtered image. Linear features such as roads are also well preserved by the filter. The filtered dataset does contain some commission errors where trees were not entirely removed. These errors show up as mottled areas on the otherwise smooth topographic surface and probably represent bushes beneath the tree canopy [Fig. 10(b)].

## IX. DISCUSSION

Some LIDAR measurements are removed in generating a regularly spaced minimum elevation grid before the progressive morphological filter is applied to the points. The disadvantage of this implementation is that good ground measurements are removed when a cell includes more than one point. This problem can be minimized by selecting a grid cell size smaller than the point spacing. The removed ground points usually have little effect on DTM generation because LIDAR measurements are so dense in space that major topographic features are rarely missed. The advantage of preprocessing the LIDAR data to generate a minimum elevation grid is that the algorithm implementation is made easier by using arrays. In addition, the dataset including multireturns can be handled by selecting a point of minimum elevation in a cell because the lowest point is more likely to be a ground measurement.

The time of filtering increases linearly as the total number of LIDAR measurements increases based on (8). Computation becomes time-consuming when the number of LIDAR measurements is large. It is impractical to apply the progressive morphological filter to process all measurements as a single file because millions of points were collected for each survey. For efficient processing, the data can be split into tiles with a user-specified size, and then the filter is applied to these tiles.

LIDAR data sometimes may contain a few points with large negative elevation values drastically lower than those of their neighbors. These measurements are called negative blunders, and their source is still in debate [8]. The proposed progressive morphological filter cannot remove negative blunders by only performing the opening operation. When a DTM is interpolated using the ground measurements including negative blunders, conical pits like “bomb craters” [8] will be generated. Fortunately, a negative blunder is distinctive from their surroundings in elevation and occupies a small area in space (often as an individual point). Therefore, it can be removed by performing a closing operation immediately following a series of opening operations that are applied to the LIDAR dataset as described previously. The closing operation could diminish the details of terrain by removing low-elevation objects less than the window size. However, the terrain reduction will be minor because only a small size window is used in the closing operation.

## X. CONCLUSIONS

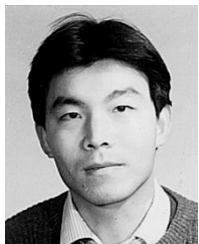
A progressive morphological filter was built to remove nonground LIDAR measurements to generate bare-ground elevation models. Experimental results show that the proposed progressive morphological filter separated ground and nonground LIDAR measurements in both the urban and mountain areas accurately and effectively by gradually increasing the sizes of the opening operation and using elevation difference threshold. The

accuracy analysis of filtering results for the urban dataset shows that only 3% errors were committed by the filter in a random sample of 648 measurements.

The selections of the filtering parameters have a great impact on the removal of nonground objects. Appropriate parameters can be found based on analyzing terrain and nonterrain measurements in the study area. The filtering process is highly automatic and requires little human interference, which is desirable when processing voluminous LIDAR measurements. However, this method is not perfect, and a few commission and omission errors did occur during filtering. A human interactive filtering method may need to be developed in the future to refine the filtering results.

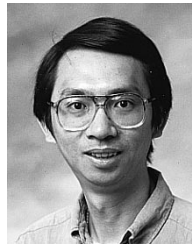
#### REFERENCES

- [1] K. Kraus and N. Pfeifer, "A new method for surface reconstruction from laser scanner data," *Int. Arch. Photogramm. Remote Sens.*, pt. 3-2W3, vol. 32, 1997.
- [2] —, "Determination of terrain models in wood areas with airborne laser scanner data," *ISPRS J. Photogramm. Remote Sens.*, vol. 53, pp. 193-203, 1998.
- [3] N. Pfeifer, P. Stadler, and C. Briese, "Derivation of digital terrain models in the SCOP++ environment," in *Proc. OEEPE Workshop on Airborne Laserscanning and Interferometric SAR for Digital Elevation Models*, Stockholm, Sweden, 2001.
- [4] G. Vosselman, "Slope based filtering of laser altimetry data," *Int. Arch. Photogramm. Remote Sens.*, pt. B4, vol. 33, pp. 958-964, 2000.
- [5] R. G. Congalton, "A review of assessing the accuracy of classifications of remotely sensed data," *Remote Sens. Environ.*, vol. 37, pp. 35-46, 1991.
- [6] M. Roggero, "Airborne laser scanning: Clustering in raw data," *Int. Arch. Photogramm. Remote Sens.*, pt. 3/W4, vol. 34, pp. 227-232, 2001.
- [7] G. Sithole, "Filtering of laser altimetry data using a slope adaptive filter," *Int. Arch. Photogramm. Remote Sens.*, pt. 3/W4, pp. 203-210, 2001.
- [8] R. A. Haugerud and D. J. Harding, "Some algorithms for virtual deforestation (VDF) of LIDAR topographic survey data," *Int. Arch. Photogramm. Remote Sens.*, pt. 3/W4, vol. 34, pp. 211-218, 2001.
- [9] P. Axelsson, "DEM generation from laser scanner data using adaptive tin models," *Int. Arch. Photogramm. Remote Sens.*, pt. B3, vol. 33, pp. 85-92, 2000.
- [10] J. Kilian, N. Haala, and M. English, "Capture and evaluation of airborne laser scanner data," *Int. Arch. Photogramm. Remote Sens.*, vol. 31, pp. 383-388, 1996.
- [11] P. Lohmann, A. Koch, and M. Schaeffer, "Approaches to the filtering of laser scanner data," *Int. Arch. Photogramm. Remote Sensing*, pt. B3, vol. 33, pp. 540-547, 2000.
- [12] R. M. Haralick and L. G. Shapiro, *Computer and Robot Vision*. Reading, MA: Addison-Wesley, 1992, vol. 1.
- [13] R. M. Haralick, S. R. Sternberg, and X. Zhuang, "Image analysis using mathematical morphology," *IEEE Trans. Pattern Anal. Machine Intell.*, vol. PAMI-9, pp. 523-550, 1987.
- [14] W. Eckstein and O. Munkelt, "Extracting objects from digital terrain models," in *Proc. Int. Society for Optical Engineering: Remote Sensing and Reconstruction for Three-Dimensional Objects and Scenes*, 1995.
- [15] H. Wackernagel, *Multivariate Geostatistics*. Berlin, Germany: Springer-Verlag, 1998.
- [16] S. P. Kaluzny, S. C. Vega, T. P. Cardoso, and A. A. Shelly, *S+Spatial-Stats: User's Manual for Windows and UNIX*. New York: Springer-Verlag, 1997.



**Keqi Zhang** received the Ph.D. degree from the Department of Geography, University of Maryland, College Park, 1998.

Since 1999, he has been a Research Assistant Professor in the International Hurricane Center, Florida International University, Miami. His research interests include airborne LIDAR mapping, 3-D Visualization and GIS. He has authored and coauthored 15 papers in journals. Currently, he is leading a team to develop the high-resolution storm surge model and 3-D animation of storm surge flooding.



**Shu-Ching Chen** (S'95-M'01) received the M.S. degrees in computer science, electrical engineering, and civil engineering and in 1998 the Ph.D. degree, all from Purdue University, West Lafayette, IN.

He is currently the Director of the Distributed Multimedia Information System Laboratory and the Associate Director of the Center for Advanced Distributed System Engineering at Florida International University (FIU), Miami. Since 1999, he has been an Assistant Professor in the School of Computer Science, FIU. Before joining FIU, he worked as a Research and Development Software Engineer for the database engine design group at Micro Data Base Systems, Inc., West Lafayette, IN. His main research interests include distributed multimedia database systems, data mining, and GIS. He has authored and coauthored one book and more than 80 research papers in journals, refereed conference proceedings, and book chapters.

Dr. Chen was the program Co-Chair of the 10th ACM International Symposium on Advances in Geographic Information Systems.



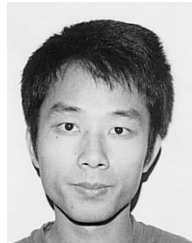
**Dean Whitman** received the Ph.D. degree in geophysics from the Department of Geological Sciences, Cornell University, Ithaca, NY, in 1993.

He is currently an Associate Professor in the Department of Earth Sciences, Florida International University, Miami. He specializes in geophysics, remote sensing, and GIS.

**Mei-Ling Shyu** (S'95-M'99) received the M.S. degrees in computer science, electrical engineering, and restaurant, hotel, institutional, and tourism management in 1992, 1995, and 1997, respectively, and the Ph.D. degree in 1999, all from Purdue University, West Lafayette, IN.

Since 2000, she has been an Assistant Professor at the Department of Electrical and Computer Engineering, University of Miami, Coral Gables, FL. Her research interests include data mining, GIS, multimedia database systems, multimedia information systems, multimedia networking, and database systems. She has authored and coauthored more than 60 technical papers published in various prestigious journals, referred conference proceedings, and book chapters.

Dr. Shyu has served on the program committee of several conferences, including the 10th ACM International Symposium on Advances in Geographic Information Systems.



**Jianhua Yan** received the M.S. degree from the Institute of Image Processing and Pattern Recognition, Shanghai Jiaotong University, Shanghai, China, in 2000. He is currently pursuing the Ph.D. degree at the School of Computer Science, Florida International University, Miami.

His research interests include image processing, pattern recognition, GIS, and neural networks.



**Chengcui Zhang** (S'03) received the B.S. and M.S. degrees in computer science from Zhejiang University, Zhejiang, China, in 1996 and 1999. She is currently pursuing the Ph.D. degree at the School of Computer Science, Florida International University (FIU), Miami. Her current research interests include multimedia database systems, multimedia data mining, video segmentation and indexing, and content-based image retrieval.

Ms. Zhang was awarded the Presidential Fellowship from FIU in 2001.